

## Constraints on the composition of the Aleutian arc lower crust from $V_P/V_S$

Donna J. Shillington,<sup>1</sup> Harm J. A. Van Avendonk,<sup>2</sup> Mark D. Behn,<sup>3</sup> Peter B. Kelemen,<sup>1</sup> and Oliver Jagoutz<sup>4</sup>

Received 10 December 2012; revised 15 March 2013; accepted 15 March 2013; published 7 June 2013.

[1] Determining the bulk composition of island arc lower crust is essential for distinguishing between competing models for arc magmatism and assessing the stability of arc lower crust. We present new constraints on the composition of high  $P$ -wave velocity ( $V_P=7.3\text{--}7.6$  km/s) lower crust of the Aleutian arc from best-fitting average lower crustal  $V_P/V_S$  ratio using sparse converted  $S$ -waves from an along-arc refraction profile. We find a low  $V_P/V_S$  of  $\sim 1.7\text{--}1.75$ . Using petrologic modeling, we show that no single composition is likely to explain the combination of high  $V_P$  and low  $V_P/V_S$ . Our preferred explanation is a combination of clinopyroxenite ( $\sim 50\text{--}70\%$ ) and alpha-quartz bearing gabbros ( $\sim 30\text{--}50\%$ ). This is consistent with Aleutian xenoliths and lower crustal rocks in obducted arcs, and implies that  $\sim 30\text{--}40\%$  of the full Aleutian crust comprises ultramafic cumulates. These results also suggest that small amounts of quartz can exert a strong influence on  $V_P/V_S$  in arc crust. **Citation:** Shillington, D. J., H. J. A. Van Avendonk, M. D. Behn, P. B. Kelemen, and O. Jagoutz (2013), Constraints on the composition of the Aleutian arc lower crust from  $V_P/V_S$ , *Geophys. Res. Lett.*, 40, 2579–2584, doi:10.1002/grl.50375.

### 1. Introduction

[2] Competing models for arc magmatism make different predictions for the thickness and composition of arc lower crust [e.g., *DeBari and Sleep*, 1991]. Information on the composition of arc lower crust is also needed to estimate its long-term stability [*Jull and Kelemen*, 2001; *Behn and Kelemen*, 2006]. To reconcile the average “andesitic” composition of continental crust with primitive island arc compositions, many models call for foundering of dense mafic-ultramafic cumulates into the underlying mantle [e.g., *Arndt and Goldstein*, 1989; *Kay and Kay*, 1993].

[3] However, constraining the composition of the island arc lower crust and distinguishing high-velocity lower crust from upper mantle rocks is difficult because (1) lower crustal arc sections are poorly represented in obducted sections [*Kelemen et al.*, 2003a and references therein]; (2) the

primary constraints on the lower crust and upper mantle in many active arcs are xenoliths and  $P$ -wave velocities ( $V_P$ ). It is unclear how representative the former may be, and the latter cannot uniquely distinguish between the effects of composition, temperature and melt. For example,  $V_P$  of  $7.x$  km/s beneath the Izu-Bonin-Marianas arc are interpreted to represent hot mantle, possibly with melt [*Suyehiro et al.*, 1996] or ultramafic cumulates [*Kodaira et al.*, 2007]. Even in the absence of elevated temperatures and/or melt,  $V_P$  cannot be used to differentiate between different possible lower crustal compositions [e.g., between garnet bearing and plagioclase-free compositions, *Behn and Kelemen*, 2003; *Müntener and Ulmer*, 2006] and/or serpentinized peridotite [e.g., *Lizarralde et al.*, 2002].

[4] Ambiguity in constraining the composition of the deep parts of island arcs with seismic velocities can be reduced by incorporating information on  $S$ -wave velocity ( $V_S$ ) and  $V_P/V_S$  ratios [e.g., *Christensen*, 1996]. Here, we combine an analysis of sparse  $S$ -wave data from the central Aleutian arc and petrologic modeling to better constrain the composition of the lower crust.

### 1.1. Existing Constraints on Compositions in the Central Aleutian Arc

[5] Aleutian volcanic rocks exhibit a spectrum of compositions (high-Al basalts, high-Mg basalts, and andesites) and fractionation trends (calc-alkaline and tholeiitic); this compositional diversity has been attributed to variations in fractionation depth, state of stress in the overriding plate, differences in parental magma compositions, and water content [*Kay et al.*, 1982; *Myers*, 1988; *Singer and Myers*, 1990; *Miller et al.*, 1992; *Sisson and Grove*, 1993a; *Kelemen et al.*, 2003b; *Zimmer et al.*, 2010]. These models make different predictions for lower crustal composition. For example, one explanation for the abundance of high-Al basalts is the crystallization of a thick sequence of pyroxenite at depth (possibly due to the presence of water), which would enrich the remaining liquid in Al [*Sisson and Grove*, 1993a]. The mineral assemblages of lower crustal rocks may also be modified following crystallization by metamorphism, particularly the formation of garnet [*Behn and Kelemen*, 2006]. The only direct information on the Aleutian lower crust comes from limited xenoliths, many of which are (olivine-) clinopyroxenites [*Conrad et al.*, 1983; *DeBari et al.*, 1987; *Yogodzinski and Kelemen*, 2007], but it is not clear how representative these are.

[6] Existing active-source seismic data from the Central Aleutians acquired in 1994 with the R/V *Maurice Ewing* and onshore/offshore seismometers (Figure 1) indicate relatively high  $V_P$  in the lower crust of the Aleutian arc [*Holbrook et al.*, 1999; *Lizarralde et al.*, 2002; *Shillington et al.*, 2004; *Van Avendonk et al.*, 2004]. For the lower crust of the oceanic island arc, these range from  $\sim 7.0\text{--}7.1$  km/s

Additional supporting information may be found in the online version of this article.

<sup>1</sup>Lamont-Doherty Earth Observatory of Columbia University, Palisades, New York, USA.

<sup>2</sup>Institute for Geophysics, University of Texas, Austin, Texas, USA.

<sup>3</sup>Woods Hole Oceanographic Institution, Woods Hole, Massachusetts, USA.

<sup>4</sup>Massachusetts Institute of Technology, Boston, Massachusetts, USA.

Corresponding author: D. J. Shillington, Lamont-Doherty Earth Observatory of Columbia University, Palisades, NY USA. (djs@ldeo.columbia.edu)

©2013. American Geophysical Union. All Rights Reserved. 0094-8276/13/10.1002/grl.50375

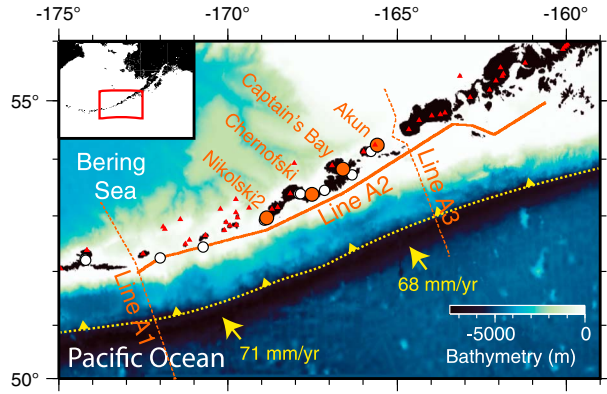


**Figure 1.** Map with 1994 Aleutian experiment. Bold orange line shows shotline used in this study. Instruments shown with white circles; instruments whose data are used here shown with orange circles and text. Red triangles indicate volcanoes from the Smithsonian Global Volcanism Program. Plate boundary and convergence directions and rates with respect to North American shown with yellow dotted lines, arrows and text [DeMets *et al.*, 2010].

directly beneath the active arc [Holbrook *et al.*, 1999] to 7.3–7.6 km/s slightly trenchward [Shillington *et al.*, 2004]. There is a sharp step in velocity at the top of the lower crust ( $\sim 0.4$  km/s), and along-arc variations in lower crustal velocity appear to correlate to variations in lava composition [Shillington *et al.*, 2004]. These characteristics were attributed to mafic/ultramafic cumulates and/or garnet granulites in the lower crust [Shillington *et al.*, 2004], but  $V_P$  alone cannot distinguish between different possible lower crustal compositions and other explanations, such as partial melt in the subarc mantle or serpentinized mantle in the forearc mantle wedge.

## 1.2. Analysis of $S$ -wave Arrivals

[7] To constrain the  $V_P/V_S$  ratio of the deep Aleutian arc crust, we performed a very simple analysis of sparse converted  $S$ -wave arrival times from the arc-parallel wide-angle seismic profile acquired in 1994. Seismometers on the Aleutian Islands recorded shots from the 8000 in<sup>3</sup> airgun array of the R/V *Maurice Ewing*, which steamed south of the islands (Figure 1). Thus, the majority of  $P$ - and  $S$ -wave ray paths in this experiment sampled the arc crust trenchward of the active arc, but were still within the arc platform [Shillington *et al.*, 2004; Van Avendonk *et al.*, 2004].

[8] We focus our analysis on arrivals from four stations where converted  $S$ -wave reflections and refractions were observed at large enough shot-receiver offsets to sample much of the crust (Figure 1). Arrivals occur over source-receiver offsets of 20–180 km and have apparent velocities from  $\sim 3$  to 4.2 km/s (Figure 2). Consistent with the observation of distinct  $P$ -wave reflections and refractions from three laterally continuous layers, we identify three crustal  $S$ -wave refractions with distinct apparent velocities; intracrustal and Moho  $S$ -wave reflections are also observed (Figure 2 and auxiliary material). Upper crustal arrivals have comparatively 3-D paths due to the experiment geometry, but the longer ray paths of lower crustal refractions and Moho reflections approximately fall in the 2-D plane along the arc platform (Figure 1). Our analysis included 2306 picks; they have large uncertainties ( $\sim 150$ –500 ms) because they

occur in the coda of the  $P$ -wave arrivals. Raytracing tests suggest that  $P$ -to- $S$  conversions occurred at the seafloor or at the top of basement beneath a thin veneer of sediments.

[9]  $S$ -wave arrivals were previously identified in this data set by Fliedner and Klemperer [1999], who used travel times in independent 3-D  $P$ - and  $S$ -wave tomographic inversions. We argue that the paucity of  $S$ -wave observations and large uncertainties in travel time picks favor an alternate, simpler analysis approach. We searched for the best-fitting, constant  $V_P/V_S$  ratio for each layer. An  $S$ -wave model was calculated from the  $P$ -wave model for each of a range of  $V_P/V_S$  ratios. We traced rays through each model in 3-D to produce predicted arrivals times for reflections and refractions, which were used to calculate a RMS misfit. Starting with the upper crust and working down, we found the best-fitting constant  $V_P/V_S$  ratio for each layer. A fixed delay of 1.8 s was used to account for structure beneath the stations; a similar approach was used for the  $P$ -wave modeling [Van Avendonk *et al.*, 2004].

## 1.3. Results of $S$ -wave Modeling

[10] This approach yielded ranges of best-fitting constant  $V_P/V_S$  for the upper, middle and lower crust along the central Aleutian island arc. Here we focus on results for the lower crust. The RMS misfit curve for  $S$ -wave refractions within the lower crust and reflections off the base of the lower crust (i.e., the Moho) shows a clear minimum at a  $V_P/V_S$  of 1.70 (Figure 3). Given the large uncertainties associated with travel time picks of these sparse data and the simple approach taken here, models with  $V_P/V_S$  between  $\sim 1.65$

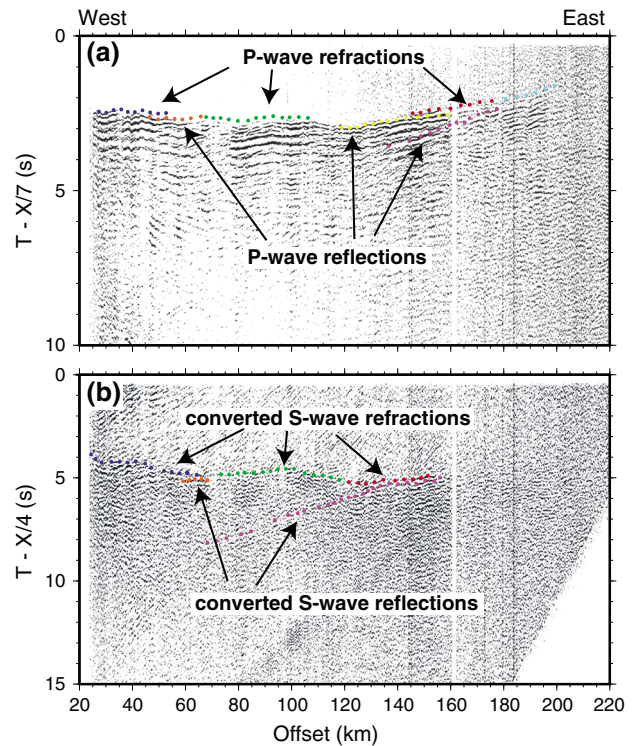


**Figure 2.** Data from Nikol'ski2 (location in Figure 1). (a)  $P$ -wave arrivals in section reduced at 7 km/s. (b) Converted  $S$ -wave arrivals in same data reduced at 4 km/s. Refractions from upper (blue), middle (green), lower crust (red), and upper mantle (turquoise). Reflections from base of upper (orange), middle (yellow), and lower crust (purple).

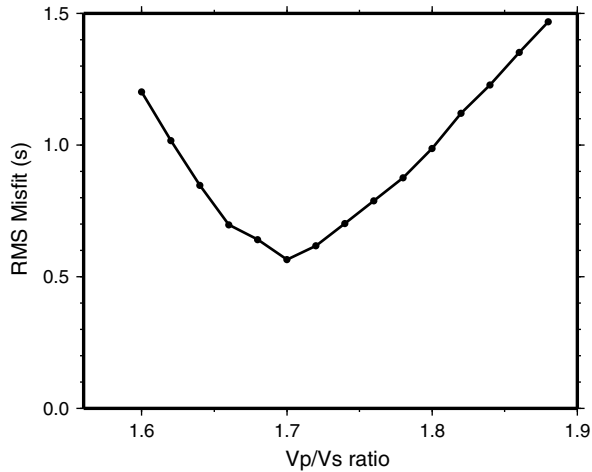


**Figure 3.** RMS residuals for various lower crustal  $V_P/V_S$  for  $S$ -arrivals on instruments shown in Figure 1.

and 1.75 are considered acceptable. However, the apparent velocities of the refractions, alone, indicate a higher  $V_P/V_S$  ( $\sim 1.75$ ). Additionally, the average lower crustal  $V_P/V_S$  based on regional earthquakes indicates a  $V_P/V_S$  of  $\sim 1.74$ – $1.77$  [Abers, 1994], and higher lower crustal  $V_P/V_S$  are implied in the lower crust directly beneath the active arc by receiver functions at stations along the arc (H. A. Janiszewski *et al.*, 2013, submitted). Thus, we favor the upper end of our acceptable range (1.7–1.75).

#### 1.4. Interpretation of $V_P/V_S$

[11] The new  $V_P/V_S$  results presented here combined with the  $V_P$  model along the same profile [Shillington *et al.*, 2004; Van Avendonk *et al.*, 2004] provide unique new constraints on island arc lower crust. Below we discuss different possible explanations for our observations.

[12] Although the range of permissible average  $V_P/V_S$  ratios from our study is large, it immediately excludes many possible explanations for  $7.x$  km/s  $P$ -wave velocities in the lower crust and/or upper mantle. If  $P$ -wave velocities of  $7.3$ – $7.6$  km/s were caused by serpentinization of the mantle wedge approaching the forearc, we would expect relatively high  $V_P/V_S$  [e.g., Christensen, 2004, Figure 4]. Likewise, high temperatures and the presence of melt would also increase  $V_P/V_S$  [e.g., Faul and Jackson, 2005]. Anisotropy can also influence the estimation of  $V_P/V_S$  [Hacker and Abers, 2012]. However, for the ray paths in this study and possible mineral assemblages in the lower crust, we infer that anisotropy is unlikely to completely account for the observed low  $V_P/V_S$ .

[13] In general, the dominant compositional control on  $V_P/V_S$  variations in the crust is silica content; higher silica rocks are generally associated with lower  $V_P/V_S$  [Christensen, 1996, Figure 4]. However, in mafic and ultramafic rocks with low  $\text{SiO}_2$ , other minerals begin to play a role in controlling the velocity characteristics. There are several possible constituent minerals that could be present in the Aleutian lower crust that would result in a relatively low  $V_P/V_S$  ( $< 1.75$ ).

[14] Pyroxenite can have  $V_P/V_S$  ranging from  $\sim 1.68$  to  $1.85$  (Figure 4), depending on the composition of the pyroxenite (orthopyroxene has a lower  $V_P/V_S$  than clinopyroxene) [Behn and Kelemen, 2006]. Many xenoliths from the Aleutians are (olivine-) clinopyroxenites [Conrad

*et al.*, 1983; Conrad and Kay, 1984; DeBari *et al.*, 1987; Yagodinski and Kelemen, 2007]. The estimated  $V_P$  of these compositions based on Hacker and Abers [2004] ( $\sim 7.5$ – $7.8$  km/s) is at the upper end of the  $V_P$  range for the lower crust from Shillington *et al.* [2004] ( $7.3$ – $7.6$  km/s), but the  $V_P/V_S$  ratio ( $\sim 1.77$ – $1.79$ ) is higher than the values presented here (Figure 4). Thus, another composition must be present in addition to (or instead of) clinopyroxenite.

[15] Orthopyroxene has a lower  $V_P/V_S$  ratio and could be present due to the breakdown of olivine plus plagioclase to form clinopyroxene, orthopyroxene, and spinel [Kushiro and Yoder, 1966]. Alternatively, metasomatism of olivine-rich rocks by silicious fluids can form orthopyroxene at temperatures above serpentinite stability but below the solidus ( $\sim 700$ – $1000^\circ\text{C}$ ) [Wagner *et al.*, 2008]. Orthopyroxenite could fit our observed  $V_P$  and  $V_P/V_S$  (Figure 4); however, orthopyroxene is not observed in any of the lower crustal or upper mantle xenoliths from the Aleutians [Conrad *et al.*, 1983; DeBari *et al.*, 1987]. Therefore, although orthopyroxene may be present, we find it unlikely that it forms in sufficient abundances to explain the observed  $V_P/V_S$  ratios.

[16] Another possible contribution to low  $V_P/V_S$  is the presence of quartz. Quartz is common in felsic and intermediate arc rocks. Its presence in more mafic rocks could occur due to fluxing of silicious material from the slab [Rossi *et al.*, 2006]. Alternatively, the metamorphic reaction of enstatite and plagioclase forms garnet, clinopyroxene and quartz [Kushiro and Yoder, 1966]. The abundance of quartz in the deep Aleutian crust is unknown; Conrad *et al.* [1983] reported that a gabbroic xenolith from Adak contains quartz. It is also observed in deep crustal rocks from the obducted Kohistan arc [Yamamoto, 1993; Jagoutz and Schmidt, 2012], but is not observed in lower crustal gabbroites in the Talkeetna section [Kelemen *et al.*, 2003a; Behn and Kelemen, 2006]. The elastic properties of quartz change dramatically with the transition from alpha to beta quartz; alpha quartz has a much lower  $V_P/V_S$  ( $\sim 1.4$ ) than beta quartz ( $\sim 1.7$ ) [e.g., Ohno *et al.*, 2006]. The profound effect of the alpha-beta quartz transition is illustrated in Figure 4, which shows  $V_P$  and  $V_P/V_S$  calculated using *Perple\_X* [Connolly, 2005] for rocks from obducted arc sections in Talkeetna and Kohistan at 0.8 GPa (see auxiliary material). Calculations at  $750^\circ\text{C}$  lie within the alpha quartz stability field, and rocks with higher  $\text{SiO}_2$  trend toward low  $V_P$  and low  $V_P/V_S$  ratios (Figure 4a). By contrast, velocities calculated at  $900^\circ\text{C}$  lie within the beta quartz stability field, and rocks with higher  $\text{SiO}_2$  trend toward low  $V_P$  and high  $V_P/V_S$  (Figure 4b). Our rays sample the lower crust trenchward of the active arc line, where colder temperatures are expected, making the stability of alpha quartz more plausible [Shen *et al.*, 1993].

[17] The sensitivity of the expected mineral assemblages arising from different bulk compositions as a function of temperature and pressure was assessed by examining several possible lower crustal compositions derived from obducted arc sections using *Perple\_X* (see auxiliary material). To satisfy the high  $V_P$  in the Aleutian lower crust, the presence of quartz, which has low  $V_P$ , would need to be balanced by other components with higher  $V_P$ , such as garnet. The pressure-temperature window in which both phases are stable is either nonexistent or very narrow and confined to conditions only present in the lowermost Aleutian crust (Figure S7). Consequently, we conclude that alpha quartz

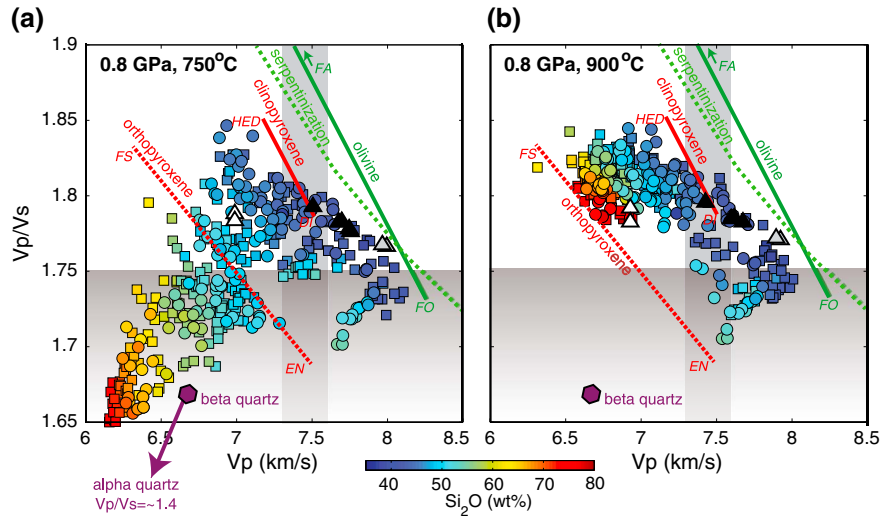


**Figure 4.** Seismic velocities of obducted arc rocks from Talkeetna and Kohistan [Kelemen *et al.*, 2003a; Jagoutz *et al.*, 2006]. Phase proportions and velocities were calculated from bulk composition with a version of Perple\_X modified to include the alpha/beta quartz transition at (a) 750°C and (b) 900°C, which lie in the alpha and beta quartz stability fields, respectively. Squares are ultramafic rocks, and circles are gabbros. We assume gabbros contain 0.5 wt % H<sub>2</sub>O and ultramafic rocks are dry. Grey, black, and white triangles are velocities estimated for (olivine-) pyroxenites, dunites, and other compositions (amphibolites and hornblendites) from Aleutian xenoliths, respectively [DeBari *et al.*, 1987] using Hacker and Abers [2004]. Grey bands show range of  $V_P$  from Shillington *et al.* [2004] and  $V_P/V_S$  from this study. Lines and text indicate  $V_P$  and  $V_P/V_S$  for compositional end-members of olivine (FO-fosterite, FA-fayalite), clinopyroxene (DI-diopside, HED-hedenbergite), and orthopyroxene (EN-enstatite, FS-ferrosillite) from Hacker and Abers [2004]. Serpentinite calculated at 600°C. Almost no compositions fall within observed  $V_P$  and  $V_P/V_S$  ranges for the Aleutian lower crust, suggesting that a mixture of compositions is required.

could contribute to the observed velocity properties of some parts of the crust, but cannot be the sole explanation for the low  $V_P/V_S$  ratios over the entire Aleutian lower crust.

[18] Based on the factors discussed above, it does not appear that a single composition can fully explain the  $V_P$  and  $V_P/V_S$  of the Aleutian lower crust, but rather a combination of rock types is required. We favor the interpretation that there is abundant (olivine-) clinopyroxenite in the Aleutian lower crust, consistent with Aleutian xenoliths. These compositions have  $V_P$  that fall within the upper end of the range of  $V_P$  observed in the lower crust here, but their estimated  $V_P/V_S$  ratios are above the observed range (Figure 4). This requires that other compositions with lower  $V_P$  and  $V_P/V_S$  must also be present to account for the combination of high  $V_P$  and low  $V_P/V_S$ . Specifically, we favor mixtures that include compositions with a small amount (<5 wt %) of alpha quartz, such as rocks with ~50–65 wt % SiO<sub>2</sub> (Figure 4). Mixtures with ~30–50% alpha-quartz bearing gabbro ( $V_P=7.1$  km/s and  $V_P/V_S=1.72$ ) and ~50–70% clinopyroxenite ( $V_P=7.6$  km/s and  $V_P/V_S=1.775$ ) could account for our observations.

## 2. Discussion

[19] We analyzed *S*-wave arrivals to better constrain the composition of the deep part of the Aleutian arc, which includes a thick layer with  $V_P$  of 7.3–7.6 km/s [Shillington *et al.*, 2004]. We find relatively low  $V_P/V_S$  values of ~1.7–1.75 for this layer, which is consistent with abundant clinopyroxenite (as indicated by Aleutian xenoliths) in addition to another composition with lower  $V_P$  and lower  $V_P/V_S$  ratios. We favor gabbro or another evolved composition with small

amounts (<5%) of alpha quartz. The pressures and temperatures expected across the arc crustal section from the active arc toward the trench span the alpha-beta quartz boundary, such that even small amounts of quartz could result in large changes in  $V_P/V_S$  in the middle and lower crust across island arcs.

[20] We use lower crustal  $V_P$  and  $V_P/V_S$  to estimate that ~50–70% of the lower crust is composed of clinopyroxenite, implying that it forms ~30–40% of the entire Aleutian crustal section. The portion of the Aleutian crust comprising ultramafic cumulates is larger than the proportion of equivalent compositions exposed in obducted arcs, but similar to estimates of their proportions based on geobarometry and mass balances [Kay and Kay, 1985; DeBari and Sleep, 1991; Greene *et al.*, 2006; Jagoutz and Schmidt, 2012]. In contrast to what is interpreted for many other island arcs, we interpret the presence of significant ultramafic cumulates above the seismic Moho, and that our Moho represents the contact between mafic-ultramafic cumulates and mantle. In many arcs, these compositions are inferred to lie beneath the seismic Moho; their high velocities might make them indistinguishable from hot upper mantle, such that the Moho might instead represent a boundary between plagioclase-bearing and ultramafic compositions [Müntener and Ulmer, 2006; Kodaira *et al.*, 2007; Tatsumi *et al.*, 2008].

[21] The presence of abundant clinopyroxenite in the Aleutian lower crust can explain several key characteristics of Aleutian lavas. The crystallization of a thick layer of pyroxenite will result in a higher-Al liquid and could account for high-Al basalts in the Aleutians [Sisson and Grove, 1993a; Müntener *et al.*, 2001]. Likewise, the

depletion of the remaining melt in Fe could explain calc-alkaline fractionation trends [Sisson and Grove, 1993b; Zimmer et al., 2010]. The presence of water in the parental magma suppresses plagioclase, which can enable the crystallization of thick sections of pyroxenite and a more abrupt “plag-in” [Müntener et al., 2001]. Approximately 3–4 wt % H<sub>2</sub>O is estimated for lavas in the oceanic Aleutian arc from melt inclusions [Zimmer et al., 2010]. Simple petrological modeling suggests that the suppression of plagioclase crystallization due to the presence of water may partially account for the sharp step in  $V_P$  at the top of the lower crust in the Aleutians (Figure S8). However, our interpretation of multiple compositions in the lower crust implies that magmas undergo varied crystallization sequences during their ascent, which may also help explain the compositional diversity observed at volcanoes.

### 3. Conclusions

[22] The analysis of sparse converted *S*-waves in an along-arc refraction profile in the Aleutian island arc yields low average  $V_P/V_S$  ratios for the lower crust. The combination of high  $V_P$  and low  $V_P/V_S$  is best explained by a combination of abundant clinopyroxenite and another mafic composition containing alpha quartz. This interpretation is consistent with Aleutian xenoliths, obducted arc sections, and many petrological models for Aleutian magmas. Better constraints on *S*-wave velocity in the Aleutians and other arcs can greatly improve our knowledge of arc crustal composition.

[23] **Acknowledgments.** We gratefully acknowledge B. Hacker, G. Abers and H. Janiszewski for discussions, J. Connolly for help with *Perple\_X*, and M. Fliedner and S. Klemperer for providing information on the Aleutians Experiment. PBK's contributions supported by the Arthur D. Storke Chair at Columbia University and by NSF grants OCE 0520378, OCE 0728077, and EAR 0727013. The constructive suggestions of two anonymous reviewers and A. Newman greatly improved the manuscript.

### References

Abers, G. A. (1994), Three-dimensional inversion of regional P and S arrival times in the East Aleutians and sources of subduction zone gravity highs, *J. Geophys. Res.*, *99*(B3), 4395–4412.

Arndt, N. T., and S. L. Goldstein (1989), An open boundary between continental crust and mantle: its role in crust formation and crustal recycling, *Tectonophysics*, *161*, 201–212.

Behn, M. D., and P. B. Kelemen (2003), Relationship between seismic P-wave velocity and the composition of anhydrous igneous and meta-igneous rocks, *Geochem. Geophys. Geosys.*, *4*(5), 1041, doi:10.1029/2002GC000393.

Behn, M. D., and P. B. Kelemen (2006), The stability of arc lower crust: Insights from the Talkeetna Arc section, south-central Alaska and the seismic structure of modern arcs, *J. Geophys. Res.*, *111*, B11207, doi:10.1029/12006JB00427.

Christensen, N. I. (1996), Poisson's ratio and crustal seismology, *J. Geophys. Res.*, *101*(B2), 3139–3156.

Christensen, N. I. (2004), Serpentinities, peridotites, and seismology, *Intern. Geol. Rev.*, *46*, 795–816.

Connolly, J. A. D. (2005), Computation of phase equilibria by linear programming: A tool for geodynamic modeling and its application to subduction zone decarbonation, *Earth Planet. Sci. Lett.*, *236*, 524–541.

Conrad, W. K., S. M. Kay, and R. W. Kay (1983), Magma Mixing in the Aleutian Arc: Evidence From Cognate Inclusions and Composite Xenoliths, *J. Volcanol. Geotherm. Res.*, *18*, 279–295.

Conrad, W. K., and R. W. Kay (1984), Ultramafic and Mafic Inclusions from Adak Island: Crystallization History, and Implications for the Nature of Primary Magmas and Crustal Evolution of the Aleutian Arc, *J. Petrol.*, *25*, 88–125.

DeBari, S., S. M. Kay, and R. W. Kay (1987), Ultramafic xenoliths from Adagdak Volcano, Adak, Aleutian Islands, Alaska: Deformed Igneous Cumulates from the Moho of an Island Arc, *J. Geol.*, *95*, 329–341.

DeBari, S. M., and N. H. Sleep (1991), High-Mg, low-Al bulk composition of the Talkeetna island arc, Alaska: Implications for primary magmas and the nature of arc crust, *Geol. Soc. Am. Bull.*, *103*, 37–47.

DeMets, C., R. G. Gordon, and D. F. Argus (2010), Geological current plate motions, *Geophys. J. Intl.*, *181*, 1–80.

Faul, U. H., and I. Jackson (2005), The seismological signature of temperature and grain size variations in the upper mantle, *Earth and Planetary Science Letters*, *234*, 119–134.

Fliedner, M. M., and S. L. Klemperer (1999), Structure of an island-arc: Wide-angle seismic studies in the eastern Aleutian Islands, Alaska, *J. Geophys. Res.*, *104*(B5), 10667–10694.

Greene, A. R., S. DeBari, P. B. Kelemen, J. Blusztajn, and P. D. Clift (2006), A detailed geochemical study of island arc crust: The Talkeetna Arc Section, South-central Alaska, *J. Petrol.*, *47*(6), 1051–1093.

Hacker, B. R., and G. A. Abers (2004), Subduction Factory 3: An Excel worksheet and macro for calculating the densities, seismic wave speeds, and H<sub>2</sub>O contents of minerals and rocks at pressure and temperature, *Geochem. Geophys. Geosys.*, *5*(1), Q01005, doi:10.1010.01029/2003GC000614.

Hacker, B. R., and G. A. Abers (2012), Subduction Factory 5: Unusually low Poisson's ratios in subduction zones from elastic anisotropy of peridotite, *J. Geophys. Res.*, *117*, B06308, doi:10.1029/2012JB009187.

Holbrook, W. S., D. Lizarralde, S. McGeary, N. Bangs, and J. Diebold (1999), Structure and composition of the Aleutian island arc and implication for continental crustal growth, *Geology*, *27*(1), 31–34.

Jagoutz, O., O. Müntener, J.-P. Burg, P. Ulmer, and E. Jagoutz (2006), Lower continental crust formation through focused flow in km-scale melt conduits: The zoned ultramafic bodies of the Chilas Complex in the Kohistan island arc (NW Pakistan), *Earth Planet. Sci. Lett.*, *242*, 320–342.

Jagoutz, O., and M. W. Schmidt (2012), The formation and bulk composition of modern juvenile continental crust: The Kohistan arc, *Chem. Geol.*, *298–299*, 79–96.

Janiszewski, H. A., G. A. Abers, D. Shillington, and J. A. Calkins (2013), Crustal structure along the Aleutian island arc: New insights from receiver functions constrained by active source data, *Geochem. Geophys. Geosys.*, submitted.

Jull, M., and P. B. Kelemen (2001), On the conditions for lower crustal convective instability, *J. Geophys. Res.*, *106*(B4), 6423–6446.

Kay, R. W., and S. M. Kay (1993), Delamination and delamination magmatism, *Tectonophysics*, *219*, 177–189.

Kay, S. M., R. W. Kay, and G. P. Citron (1982), Tectonic Controls of Tholeiitic and Calc-Alkaline Magmatism in the Aleutian Arc, *J. Geophys. Res.*, *87*(B5), 4051–4072.

Kay, S. M., and R. W. Kay (1985), Role of crystal cumulates and the oceanic crust in the formation of the lower crust of the Aleutian arc, *Geology*, *13*, 461–464.

Kelemen, P. B., K. Hanghøj, and A. R. Greene (2003a), One view of the geochemistry of subduction-related magmatic arcs, with an emphasis on primitive andesite and lower crust, in *The Crust*, edited by R. L. Rudnick, Elsevier, Oxford.

Kelemen, P. B., G. M. Yogodzinski, and D. W. Scholl (2003b), Along-Strike Variation in the Aleutian Island Arc: Genesis of High Mg# Andesite and Implications for Continental Crust, *Geophys. Mono. Ser.*, *138*, pp. 223–276.

Kodaira, S., T. Sato, N. Takahashi, A. Ito, Y. Tamura, Y. Tatsumi, and Y. Kaneda (2007), Seismological evidence for variable growth of crust along the Izu intra-oceanic arc, *J. Geophys. Res.*, *112*(B5), B05104.

Kushiro, I., and H. S. Yoder (1966), Anorthite-forsterite and anorthite-enstatite reactions and their bearing on basalt-eclogite transformation, *J. Pet.*, *7*(3), 337.

Lizarralde, D., W. S. Holbrook, S. McGeary, N. Bangs, and J. Diebold (2002), Crustal construction of a volcanic arc, wide-angle seismic results from the western Alaska Peninsula, *J. Geophys. Res.*, *107*(8), 2164, doi:10.1029/2001JB000230.

Miller, D. M., C. H. Langmuir, S. L. Goldstein, and A. L. Franks (1992), The Importance of Parental Magma Composition to the Calc-Alkaline and Tholeiitic Evolution: Evidence From Umnak Island in the Aleutians, *J. Geophys. Res.*, *97*(B1), 321–343.

Müntener, O., P. B. Kelemen, and T. L. Grove (2001), The role of H<sub>2</sub>O during crystallization of primitive arc magmas under uppermost mantle conditions and genesis of igneous pyroxenites: an experimental study, *Contributions to Mineralogy and Petrology*, *141*, 643–658.

Müntener, O., and P. Ulmer (2006), Experimentally derived high-pressure cumulates from hydrous arc magmas and consequences for the seismic velocity structure of island arc crust, *Geophys. Res. Lett.*, *33*(21), L21308, doi:10.1029/2006GL027629.

Myers, J. D. (1988), Possible petrogenetic relations between low- and high-MgO Aleutian basalts, *Geol. Soc. Am. Bull.*, *100*, 1040–1053.

Ohno, I., K. Harada, and C. Yoshitomi (2006), Temperature variation of elastic constants of quartz across the alpha-beta transition, *Phys. Chem. Minerals*, *33*, 1–9.

- Rossi, G., G. A. Abers, S. Rondenay, and D. H. Christensen (2006), Unusual mantle Poisson's ratio, subduction, and crustal structure in central Alaska, *J. Geophys. Res.*, *111*, B09311, doi:10.1029/2005JB003956.
- Shen, A. H., W. A. Bassett, and I.-M. Chou (1993), The alpha-beta quartz transition at high temperatures and pressures in a diamond-anvil cell by laser interferometry, *Am. Mineral.*, *78*, 694–698.
- Shillington, D. J., H. J. A. Van Avendonk, W. S. Holbrook, P. B. Kelemen, and M. J. Hornbach (2004), Composition and structure of the central Aleutian island arc from arc-parallel wide-angle seismic data, *Geochem. Geophys. Geosys.*, *5*, Q10006, doi:10.1029/2004GC000715.
- Singer, B. S., and J. D. Myers (1990), Intra-arc extension and magmatic evolution in the central Aleutian arc, *Alaska, Geology*, *18*, 1050–1053.
- Sisson, T. W., and T. L. Grove (1993a), Temperatures and H<sub>2</sub>O contents of low-MgO high-alumina basalts, *Contrib. Mineral. Petrol.*, *113*, 167–184.
- Sisson, T. W., and T. L. Grove (1993b), Experimental investigations of the role of H<sub>2</sub>O in calc-alkaline differentiation and subduction zone magmatism, *Contrib. Mineral. Petrol.*, *113*(2), 143–166.
- Suyehiro, K., N. Takahashi, Y. Arieie, Y. Yokoi, R. Hino, M. Shinohara, T. Kanazawa, N. Hirata, H. Tokuyama, and A. Taira (1996), Continental crust, crustal underplating, and low-Q upper mantle beneath an oceanic island arc, *Science*, *272*, 390–392.
- Tatsumi, Y., H. Shukuno, K. Tani, N. Takahashi, S. Kodaira, and T. Kogisa (2008), Structure and growth of the Izu-Bonin-Mariana arc crust: 2. Role of crust-mantle transformation and the transparent Moho in arc crust evolution, *J. Geophys. Res.*, *113*, B02203, doi:10.1029/2007JB005121.
- Van Avendonk, H. J. A., D. J. Shillington, W. S. Holbrook, and M. J. Hornbach (2004), Inferring crustal structure in the Aleutian island arc from a sparse wide-angle seismic dataset, *Geochem. Geophys. Geosys.*, *5*, Q08008, doi:10.1029/2003GC000664.
- Wagner, L. S., M. L. Anderson, J. M. Jackson, S. L. Beck, and G. Zandt (2008), Seismic evidence for orthopyroxene enrichment in the continental lithosphere, *Geology*, *36*(12), 935–938.
- Yamamoto, H. (1993), Contrasting metamorphic P-T-time paths of the Kohistan granulites and tectonics of the western Himalayas, *J. Geol. Soc. London*, *150*, 843–856.
- Yogodzinski, G. M., and P. B. Kelemen (2007), Trace elements in clinopyroxenes from Aleutian xenoliths: Implications for primitive subduction magmatism in an island arc, *Earth Planet. Sci. Lett.*, *256*(3–4), 617–632.
- Zimmer, M. M., T. Plank, E. H. Hauri, G. M. Yogodzinski, P. Stelling, J. Larsen, B. Singer, B. Jicha, C. Mandeville, and C. J. Nye (2010), The Role of Water in Generating the Calc-alkaline Trend: New Volatile Data for Aleutian Magmas and a New Tholeiitic Index, *J. Pet.*, *51*, 2411–2444.